https://doi.org/10.5194/egusphere-2026-2815
Preprint. Discussion started: 3 July 2026

Decoupling phosphorus availability and fixation in tropical soils: roles of iron and aluminum oxides across agroecological gradients in Nigeria

Jibrin M. Jibrin[1,2], Samuel A. Mesele[2]*, Funmilayo Ande[3], James O. Jayeola[4], Ibrahim Yusuf Ibrahim[1], Ibrahim Abdu NaAbdu[1], Abdulwahab Saliu Shaibu[1]

[1]Bayero University Kano, Kano State, Nigeria
[2]International Institute of Tropical Agriculture (IITA), Ibadan, Nigeria
[3]Institute of Agricultural Research and Training, Ibadan, Nigeria
[4]Nasarawa State University, Keffi, Nasarawa State, Nigeria

* Corresponding author: s.mesele@cgiar.org

Abstract

Phosphorus (P) deficiency and fixation are major constraints to crop productivity in tropical soils, yet their large-scale interactions remain poorly understood. This study provides a national-scale assessment of how short-range-ordered iron (Fe_{ox}) and aluminum (Al_{ox}) oxides, soil properties, and climate jointly regulate P availability across Nigeria. A total of 1,382 topsoil samples (0–20 cm), collected using a hierarchical Soils4Africa framework, were analyzed for extractable P, Fe_{ox}, Al_{ox}, soil organic carbon (SOC), texture, and pH, and integrated with precipitation data. We developed a phosphorus sorption index (PSI) to quantify fixation potential as the molar ratio of oxide abundance to available P. Soil properties varied strongly along agroecological gradients, with Fe_{ox}, Al_{ox}, SOC, precipitation, and PSI increasing from semi-arid savannas to humid forest systems, while pH declined. Contrary to the expected inverse relationship, extractable P was positively associated with Fe_{ox}, Al_{ox}, SOC, and precipitation, but negatively related to PSI. Multivariate analyses clarified this apparent paradox: SOC exerted the strongest positive effect on P availability, whereas Al_{ox} had a strong negative effect consistent with sorption, and precipitation influenced P both directly and indirectly through oxide accumulation. These results demonstrate that P availability and fixation are not simply inversely coupled but are co-regulated by climatic and biological processes. The PSI effectively captured spatial variation in fixation potential, with the highest values in humid regions characterized by intensive weathering. These findings highlight the dominant role of agroecological gradients in structuring P dynamics and reveal contrasting nutrient constraints across regions: oxide-rich humid soils are limited by fixation, whereas northern savannas are constrained by low inherent P. This study provides a mechanistic basis for site-specific phosphorus management and supports the development of sustainable nutrient strategies to improve P-use efficiency in tropical agroecosystems.

Keywords: Phosphorus availability; phosphorus fixation; iron and aluminum oxides; soil organic carbon; tropical soils; nutrient-use efficiency; site-specific management; Nigeria

1. Introduction

Phosphorus (P) deficiency remains one of the most persistent constraints to crop productivity in tropical soils, limiting agricultural output and contributing to food insecurity across Sub-

https://doi.org/10.5194/egusphere-2026-2815
Preprint. Discussion started: 3 July 2026

Saharan Africa (Sanchez, 2019). In many regions, particularly the Sahel, alleviating P deficiency is a prerequisite for effective use of other nutrients and for achieving sustainable yield gains (Horst et al., 2001; Jibrin et al., 2002). Unlike nitrogen, which benefits from biological fixation and atmospheric inputs, phosphorus is derived primarily from the weathering of parent material and is characterized by low mobility and slow replenishment in soils (Roy et al., 2006). These inherent constraints result in low fertilizer-use efficiency, as a substantial proportion of applied P becomes rapidly immobilized, increasing both economic costs and environmental risks associated with nutrient management.

Sorption of phosphate onto iron (Fe) and aluminum (Al) oxides and hydroxides represents a central mechanism controlling P availability in tropical soils. Both crystalline and short-range-ordered phases exhibit strong affinity for phosphate ions, forming stable inner-sphere complexes that reduce P solubility and plant availability (Parfitt, 1978; Gerard, 2016). Short-range-ordered Fe and Al oxides are particularly influential due to their high surface area and abundance of reactive sorption sites (Schwertmann and Taylor, 1989; Asomaning, 2020). Oxalate-extractable Fe and Al (Fe_{ox} and Al_{ox}) are widely used as proxies for these reactive phases and have been shown to correlate strongly with phosphorus sorption capacity in tropical soils (Borggaard, 1983; van der Zee and van Riemsdijk, 1988). However, most existing knowledge is derived from site-specific studies, leaving uncertainty about how these mineralogical controls operate across heterogeneous landscapes.

Highly weathered soils such as Ferralsols, Acrisols, and Nitisols dominate large parts of Sub-Saharan Africa and are characterized by low inherent fertility and high phosphorus fixation capacity (Buresh et al., 1997; Sanchez, 2019). In these systems, the efficiency of applied phosphate fertilizers is often low because a substantial fraction of added P is rapidly sorbed onto soil mineral surfaces (Mutwale et al., 2023). Poor fertilizer recovery contributes to persistent nutrient limitations in smallholder farming systems and reinforces low productivity and soil degradation (Roy et al., 2006; Magnone et al., 2022). At the same time, increasing evidence indicates that the relationship between oxide abundance and plant-available P is not uniformly negative. Soils with high concentrations of reactive Fe and Al phases can also exhibit relatively high levels of extractable P, reflecting the influence of organic matter inputs, microbial activity, and P recycling processes (Hinsinger, 2001; Haynes and Mokolobate, 2001; Reed et al., 2015). These observations suggest that phosphorus availability and fixation may be co-regulated by interacting climatic, biological, and mineralogical processes rather than being simply inversely coupled.

Nigeria provides a unique setting to examine these interactions across strong environmental gradients. The country spans a wide range of agroecological zones, from humid forest systems in the south to Sudan and Sahel savannas in the north, encompassing marked differences in precipitation, weathering intensity, and soil development (Yahmed, 2002). These gradients generate soils with contrasting mineralogical and chemical properties, including oxide-rich, highly weathered soils in humid regions and sandy, weakly developed soils in arid zones (FDALR, 1990). This diversity creates a natural gradient for evaluating how the balance between P supply and fixation varies across climatic and pedogenic conditions. Despite this variability, phosphorus deficiency remains widespread across Nigerian farming systems, contributing to low fertilizer-use efficiency and constrained agricultural productivity (Osemwotai et al., 2005; Rurinda et al., 2020).

Current understanding of phosphorus dynamics in Nigeria is limited by the lack of national-scale, quantitative assessments linking oxide mineralogy to P availability across agroecological

https://doi.org/10.5194/egusphere-2026-2815
Preprint. Discussion started: 3 July 2026

zones. Most studies have focused on local or experimental sites, often targeting specific soil types or management conditions (Osemwotai et al., 2005; Ibia and Udo, 1993). As a result, the extent to which phosphorus availability and fixation are coupled or decoupled across large tropical gradients remains unresolved. Addressing this gap is essential for improving fertilizer recommendations, which often remain generalized and fail to account for spatial variation in soil properties and nutrient constraints (Rurinda et al., 2020).

Recent advances in large-scale soil data collection provide new opportunities to address this challenge. Harmonized datasets generated through efforts such as the Soils4Africa project include measurements of key soil properties across diverse environmental conditions, including short-range-ordered Fe and Al oxides, soil texture, organic carbon, and plant-available phosphorus. These datasets enable integrated analysis of mineralogical, climatic, and biological controls on P dynamics at spatial scales relevant for national and regional decision-making. Understanding the spatial distribution of phosphorus fixation potential, and its interaction with P availability, is critical for developing efficient and sustainable nutrient management strategies. Identification of regions where fixation processes dominate, as opposed to areas where P supply is limiting, can support targeted interventions that improve fertilizer-use efficiency, reduce input costs, and minimize environmental impacts. Such approaches are central to sustainable intensification in tropical agroecosystems.

This study uses harmonized soil property data from the Soils4Africa project to investigate how short-range-ordered iron and aluminum oxides regulate phosphorus availability across Nigeria's agroecological landscapes. The analysis (i) quantifies relationships between oxalate-extractable Fe and Al and plant-available P while accounting for key soil properties, including pH, clay content, and soil organic carbon; (ii) develops a phosphorus sorption index (PSI) that integrates oxide abundance with available P to estimate fixation potential; and (iii) maps the spatial distribution of P fixation across agroecological zones. The study tests the hypothesis that oxide-rich soils exhibit strong sorption capacity but do not necessarily exhibit reduced P availability due to co-regulation by climatic and biological processes, that the combined abundance of short-range-ordered Fe and Al oxides provides a robust predictor of fixation potential, and that spatial patterns of P dynamics follow gradients in weathering intensity, soil properties, and climate. This work advances a mechanistic framework for understanding the co-regulation of phosphorus availability and fixation and provides a foundation for developing site-specific, sustainable phosphorus management strategies in tropical agroecosystems.

2 Methodology

2.1 Study Area

Nigeria is located in West Africa between 4°-14°N and 3°-15°E**,** covering approximately 923,770 km² of land and encompassing diverse climatic and geological environments that influence soil formation and nutrient dynamics (Yahmed, 2002; IIASA/FAO, 2012). The country spans several agro-ecological zones, including the humid forest, derived savanna, southern Guinea Savanna, northern Guinea Savanna, mid-altitude highlands, Sudan Savanna and Sahel Savanna, characterized by strong rainfall gradients from >2000 mm in the south to less than 600 mm in the northern Sahel. Figure 1 shows the agroecological zones and the dominant geological formations. Nigeria's geology is dominated by the Precambrian Basement Complex (granites, gneisses, migmatites, and schists) and several sedimentary basins, including the Niger Delta, Benue Trough, Chad Basin, Sokoto Basin, and Bida Basin (Yahmed, 2002; Tijani, 2023). Basement-derived soils are typically strongly weathered and enriched in iron and aluminium oxides, whereas soils developed on sedimentary formations often contain

https://doi.org/10.5194/egusphere-2026-2815
Preprint. Discussion started: 3 July 2026

lower sesquioxide concentrations. These environmental gradients have produced diverse soil groups, including Ferralsols, Acrisols, Lixisols, and Luvisols, whose mineralogical composition strongly influences phosphorus sorption and availability in Nigerian agricultural soils (FDALR, 1990).

2.2 Soil sampling design and field sampling procedure

Soil sampling followed the Soils4Africa field survey protocol (Huising and Mesele, 2022), which applies a standardized hierarchical sampling framework to ensure spatial representativeness across agricultural landscapes (Kempen et al., 2021). The sampling design consisted of three nested levels. Primary Sampling Units (PSUs) were defined as 2 × 2 km grid cells, within which Secondary Sampling Units (SSUs) of 1 ha were randomly selected. Within each SSU, Tertiary Sampling Units (TSUs) of 25 m² were established as the operational soil sampling plots. Within each TSU, soil samples were collected from four subsampling locations arranged in a Y-shaped configuration, consisting of one central point and three peripheral points located approximately 2 m from the centre and spaced equidistantly. Composite surface (0-20 cm) samples collected from 1382 TSUs across Nigeria (figure 1) were used for this study.

2.3 Mid-infrared (MIR) spectral analysis of soil samples

MIR spectra were collected using a Bruker ALPHA II FT-IR spectrometer equipped with a DRIFTS module, ZnSe beamsplitter, and DTGS detector. Finely ground (<0.5 mm) soil was packed into 6-mm stainless steel micro-cups and levelled with a spatula before scanning. Spectra were acquired using OPUS software over 4000–400 cm^{-1} wavenumbers, with resolution: 8 cm^{-1}, 32 co-added scans and ~1705 wavenumber data points.

According to ICRAF soil spectral library protocols (Tchikoui et al., 2019; Viscarra Rossel et al., 2016), instrument performance was routinely evaluated using a gold reflectance reference and three ICRAF calibration soils (Katumani, White Sands, Heavy Black Cracking Clay). Background spectra were collected on the gold standard and ZnSe optics were checked routinely. Data were reported as absorbance (log_{10} of inverse reflectance).

Raw spectra were visually inspected for CO_2 interference, water absorption, baseline curvature, or aberrant shapes inconsistent with typical soil MIR signatures. Suspect spectra were re-scanned. Replicate precision was assessed by computing the coefficient of variation (CV) across duplicate spectra; absorbance values with CV > 1% (Stenberg et al., 2010) were flagged as outliers and re-measured. Only spectra meeting QC thresholds were retained for modelling.

For pre-processing and chemometric modeling, OPUS spectra were exported as ASCII files and converted into a sample-by-wavenumber matrix. Pre-processing in R (version 4.4.3, R Core Team, 2024) included: rubber-band baseline correction, Savitzky–Golay (Savitzky & Golay,1964). (smoothing (11-point, 2nd-order), mean-centering and unit-variance scaling, removal of atmospheric interference regions (≈2400–2300 cm^{-1}, 1900–1800 cm^{-1}) and Savitzky–Golay derivatives to enhance spectral features

ICRAF spectral processing scripts were used for standardized treatment, including scatter correction and region selection. Calibration models were developed using Partial Least Squares (PLS) regression (Martens & Naes, 1989) and Random Forest (RF) (Breiman, 2001), with 20% hold-out validation. The MIR-DRIFTS workflow follows established chemometric best practices, enabling simultaneous prediction of multiple soil properties from high-quality reference datasets.

The calibration subset (20% of the total samples) was strategically selected using the Kennard-Stone algorithm based on the MIRS spectral data. This ensures that the full spectral variability

https://doi.org/10.5194/egusphere-2026-2815
Preprint. Discussion started: 3 July 2026

of the entire sample set was captured within the calibration subset. These selected samples were subjected to standard laboratory wet chemical analysis.

2.4 Wet Chemistry analysis of soil samples

Soil chemical and physical properties were determined using standardized analytical procedures. Soil pH was measured potentiometrically in water suspension (1:5 soil-to-solution ratio) using a calibrated glass electrode pH meter, following ISO 10390:2005, while electrical conductivity (EC) was measured in a 1:5 soil–water extract at 25 °C using a temperature-compensated conductivity meter (ISO 11265:1994). Exchangeable acidity ($H^+ + Al^{3+}$) was determined following 1 M KCl extraction and titration (McLean, 1965). Plant-available phosphorus (P) was extracted using the Mehlich III method and quantified by inductively coupled plasma optical emission spectrometry (ICP-OES) (Mehlich, 1984). Soil organic matter was determined by dry combustion at 900 °C, with organic carbon derived from total carbon measurements (Nelson & Sommers, 1996). Short-range-ordered Fe and Al were extracted using acid ammonium oxalate under dark conditions and quantified by ICP-OES, providing an estimate of reactive oxide phases (Warren, 1994). Soil texture was determined using the Bouyoucos hydrometer method, with particle-size fractions classified according to ISO 11277:2009.

2.5 Quantification of phosphorus sorption index

To quantify soil P fixation and P supply potentials, the following pedotransfer function was calculated to give the Phosphorus Sorption Index (PSI) based on the relative abundance of amorphous Al and Fe oxides to extractable phosphorus.

$$\mathrm{PSI} = \frac{\left(\frac{Al_{ox}}{27} + \frac{Fe_{ox}}{56}\right)}{\left(\frac{P}{31}\right)}$$

where:

Al_{ox}, Fe_{ox}, and P are concentrations in mg kg^{-1}, 27, 56, and 31 represent the atomic weights (g mol^{-1}) of Al, Fe, and P, respectively. This index normalizes P-sorbing mineral abundance by available P concentration, thereby providing a mechanistically meaningful indicator of soil P fixation potential. Higher PSI values indicate a greater dominance of amorphous oxides relative to available P and, consequently, a higher likelihood of P immobilization.

2.6 Statistical Analysis

Descriptive statistics were computed for all soil and climatic variables. Results are reported as mean ± standard deviation, along with sample size (N). Normality of continuous variables was evaluated using the Shapiro–Wilk test. Variables exhibiting right-skewed distributions (P, Al_{ox}, Fe_{ox}, PSI, and precipitation) were log-transformed prior to inferential analysis.

Pearson correlation coefficients were computed among variables. Multiple linear regression (MLR) was used to quantify the relative influence of soil properties and precipitation on extractable phosphorus:

$$\log(P) = \beta_0 + \beta_1 \log(Al_{ox}) + \beta_2 \log(Fe_{ox}) + \beta_3 pH + \beta_4 SOC + \beta_5 Clay + \beta_6 \log(Precip) + \beta_7 (pH \times \log(Al_{ox})) + \varepsilon$$

https://doi.org/10.5194/egusphere-2026-2815
Preprint. Discussion started: 3 July 2026

where:

β_i are regression coefficients and ε is the error term.

Structural Equation Modeling (SEM) was employed to further disentangle direct and indirect pathways influencing extractable P. The hypothesized SEM assumed that short-range-ordered Al and Fe oxides exert direct control on P availability; and soil pH and precipitation influence P indirectly by regulating oxide formation and reactivity.

Spatial Analysis and Geostatistical Modeling

All spatial analyses were conducted in UTM Zone 32N (EPSG: 32632**)** to ensure distance-based geostatistical validity.

An empirical variogram was computed for log-transformed PSI:

$$\gamma(h) = \frac{1}{2N(h)} \sum_{i=1}^{N(h)} [Z(x_i) - Z(x_i + h)]^2$$

Optimal theoretical variogram models were selected using automated fitting procedures. Ordinary kriging was applied to interpolate PSI across Nigeria:

$$\hat{Z}(x_0) = \sum_{i=1}^{n} \lambda_i Z(x_i)$$

where λ_i are kriging weights determined by the variogram model. A local neighborhood (maximum 50 nearest observations) was specified to ensure stable predictions. Geostatistical interpolation enables visualization of spatial patterns in P fixation potential and supports regional soil fertility management planning.

All analyses were conducted in ***R*** version 4.4 (R Core Team, 2023) and QGIS (version LTR 3.44.8).

3.0 Results & Discussion

3.1 Agroecological controls on soil properties and phosphorus dynamics

Soil properties exhibited strong and systematic variation across agroecological zones (AEZs), reflecting a clear gradient from the Sahel and Sudan Savanna to the Humid Forest (Tables 1 and 2). Available P increased from 8.99 mg kg^{-1} in the Sahel and 9.36 mg kg^{-1} in the Sudan Savanna to 15.56 mg kg^{-1} in the Humid Forest, with intermediate values across the Guinea and Derived Savanna zones. Oxalate-extractable Al and Fe (Al_{ox} and Fe_{ox}) followed a similar trend, increasing from 259.14 and 438.48 mg kg^{-1} in the Sahel to 1295.68 and 1666.22 mg kg^{-1} in the Humid Forest. Soil organic carbon (SOC) increased from 0.27% to 1.52%, while pH declined from 6.39 to 5.31. Precipitation increased from 714.47 mm to 2191.90 mm, closely mirroring oxide accumulation and PSI, which increased from 66.80 to 184.64. The spatial distribution of

https://doi.org/10.5194/egusphere-2026-2815
Preprint. Discussion started: 3 July 2026

these properties is shown in figures 2-4. These trends reflect increasing weathering intensity, leaching, and accumulation of secondary Fe and Al oxides under higher rainfall conditions. Tropical soil development is strongly governed by climate, particularly rainfall, which controls mineral transformation, organic matter dynamics, and nutrient redistribution (Jenny, 1941; Tardy, 1997; Sanchez, 2019). The strong AEZ effect confirmed by two-way ANOVA results (Supplementary Table S1) indicates that climate-driven pedogenesis is the dominant control on soil properties at the national scale.

3.1 Geological Influence and interaction with agroecology

Variation across geological formations was evident but less systematic than across AEZs (Table 2). Available P ranged from 7.77 mg kg^{-1} in the Chad Formation to 18.84 mg kg^{-1} in Tertiary volcanic formations, while Al_{ox} and Fe_{ox} were highest in oxide-rich formations such as Tertiary Volcanics, Asu River Group, and Nkporo Shale. PSI exceeded 200 in these formations but remained below 70 in sandy formations, indicating strong contrasts in fixation potential. Grouping formations by geological age revealed moderate differences (Table 3), with substantial within-group variability. While parent material influences baseline mineral composition, its effects are moderated by weathering and pedogenic processes. This is confirmed by the two-way ANOVA (Supplementary Table S1), which shows that geology has significant effects only on selected variables, whereas AEZ × geology interactions are highly significant for all variables ($p < 0.001$). These interactions demonstrate that the influence of parent material is strongly conditioned by agroecological context, consistent with classical soil formation theory (Jenny, 1941) and tropical weathering processes (Tardy, 1997).

3.2 Relationships among soil properties

Pearson correlation analysis revealed strong interrelationships among soil variables (Fig. 5). Available P was positively correlated with SOC ($r = 0.55$), Al_{ox} ($r = 0.35$), Fe_{ox} ($r = 0.35$), and precipitation ($r = 0.25$), while PSI was negatively correlated with P ($r = -0.18$). Strong correlations between Al_{ox} and Fe_{ox} ($r = 0.83$) and between SOC and oxide fractions reflect their shared dependence on weathering intensity and soil development. Principal component analysis (Fig. 6) further demonstrated clear clustering by agroecological zone, with Humid Forest soils associated with high precipitation, SOC, and oxide concentrations, and Sahel/Sudan soils occupying contrasting positions. Geological groupings were less distinct, reinforcing the dominant role of climate. These results show that soil properties co-vary along environmental gradients, with precipitation acting as a key driver linking oxide formation, organic matter accumulation, and soil texture.

3.3 Decoupling phosphorus availability and fixation

A key finding of this study is that phosphorus availability and fixation are not simply inversely related. Available P showed positive correlations with Al_{ox}, Fe_{ox}, SOC, and precipitation, while PSI was negatively correlated with P (Fig. 5). This indicates that oxide-rich environments can simultaneously exhibit high fixation potential and relatively higher extractable P. This apparent contradiction arises from the co-regulation of P dynamics by multiple processes. In humid environments, increased rainfall enhances both oxide formation and biological activity, leading to higher organic matter inputs and more active P cycling. Consequently, P availability reflects the balance between sorption, mineralization, and biological recycling rather than sorption alone (Hinsinger, 2001; Vance et al., 2003; Haynes and Mokolobate, 2001). The role of oxides in P fixation is well established, particularly for amorphous Fe and Al phases, which provide

https://doi.org/10.5194/egusphere-2026-2815
Preprint. Discussion started: 3 July 2026

reactive surfaces for phosphate adsorption (Parfitt, 1978; Sanyal and De Datta, 1991; Schwertmann and Taylor, 1989). However, the positive correlation between oxides and available P indicates that these processes are embedded within broader pedogenic and ecological systems.

3.4 Mechanistic controls on phosphorus availability

Multivariate analyses provided further insight into the mechanisms controlling P availability. The regression model (Table 4) explained a substantial proportion of variance (adjusted R^2 = 0.63), with SOC as the strongest positive predictor and clay content exerting a negative effect. The Humid Forest and Southern Guinea Savanna were associated with higher P levels, while Jurassic and Tertiary formations also showed positive effects. A significant Al_{ox} × pH interaction indicates that oxide-mediated sorption is influenced by soil acidity. The structural equation model (Fig. 7) further disentangled these relationships. SOC had the strongest positive direct effect on P, highlighting the role of organic matter in enhancing P availability through mineralization and competitive sorption. In contrast, Al_{ox} exerted a strong negative effect, confirming its role as a dominant sorption phase. Fe_{ox} showed a moderate positive effect, suggesting that it reflects broader pedogenic conditions rather than acting solely as a sorption agent. Precipitation played a central role, strongly influencing Al_{ox} and Fe_{ox} accumulation and exerting both direct and indirect effects on P availability. Soil pH had smaller indirect effects, primarily through its influence on oxide formation. These findings align with previous studies showing that P dynamics in tropical soils are controlled by interacting climatic, mineralogical, and biological processes (Gerard, 2016; Hinsinger, 2001).

3.5 PSI as an integrative indicator

The phosphorus sorption index (PSI) effectively integrates oxide abundance and available P, providing a robust indicator of fixation potential. Its strong increase across AEZs (Table 1 and Fig. 4) and close association with oxide concentrations demonstrate its utility for mapping fixation risk. The lack of a significant independent geological effect on PSI, combined with strong AEZ × geology interactions (Table 4), indicates that fixation potential is primarily controlled by pedogenic processes rather than parent material alone. This supports the view that P limitation intensifies with increasing weathering and oxide accumulation (Parfitt and Smart, 1978; Borggaard, 1983).

3.6 Implications for sustainable phosphorus management

The contrasting patterns observed across agroecological zones have direct implications for sustainable P management and nutrient-use efficiency in tropical agroecosystems. In humid and subhumid regions, where PSI values are high and oxide concentrations are elevated, P limitation is primarily driven by fixation processes. In these environments, improving P-use efficiency requires strategies that reduce sorption losses and enhance biological cycling. Increasing SOC is particularly critical, as it emerged as the strongest positive determinant of P availability. Organic amendments such as manure, compost, and crop residues can mitigate fixation through competitive sorption, complexation of reactive Al and Fe phases, and stimulation of microbial P mineralization (Menezes-Blackburn et al., 2018; Vanlauwe et al., 2015). Complementary practices, including localized fertilizer placement, liming to moderate soil acidity, and the use of P-efficient crop varieties, can further improve fertilizer recovery and reduce losses.

https://doi.org/10.5194/egusphere-2026-2815
Preprint. Discussion started: 3 July 2026

In contrast, soils of the Sahel and Sudan Savanna are characterized by low PSI and low inherent P levels, indicating that P limitation is primarily due to insufficient supply rather than strong sorption. In these systems, increasing P input remains essential to overcome nutrient constraints and support crop productivity. However, responses to P fertilization are often constrained by co-limitation with other nutrients, particularly nitrogen, highlighting the importance of integrated soil fertility management strategies (Kihara et al., 2020; Rurinda et al., 2020). The coexistence of fundamentally different P constraints across regions underscores the limitations of generalized fertilizer recommendations and reinforces the need for site-specific approaches tailored to local soil conditions. More broadly, these findings contribute to sustainable intensification efforts by demonstrating that improving P-use efficiency requires simultaneous consideration of mineralogical constraints, organic matter dynamics, and climatic drivers. The PSI provides a practical tool for identifying areas with high fixation risk and guiding targeted interventions. Integration of such indices with agroecological zoning and soil information systems offers a pathway toward more efficient fertilizer use, reduced environmental impacts, and improved resilience of agricultural systems.

Conclusion

This study provides a national-scale assessment of phosphorus (P) dynamics in tropical soils, showing that agroecological gradients, particularly climate-driven weathering and organic matter dynamics, are the primary controls on P availability and fixation across Nigeria. Geological effects are secondary and largely mediated through interactions with environmental conditions. The findings demonstrate that P availability and fixation are not simply inversely related but are co-regulated by mineralogical, climatic, and biological processes. Short-range-ordered aluminum plays a dominant role in P immobilization, while soil organic carbon strongly enhances P availability, highlighting the importance of organic matter in moderating P constraints. The phosphorus sorption index (PSI) developed in this study effectively captures spatial variation in fixation potential, distinguishing high-fixation humid systems from low-P, supply-limited savanna soils. These contrasting patterns indicate that P limitation arises from different mechanisms across agroecological zones and cannot be addressed through uniform fertilizer recommendations. Integrating PSI with agroecological zoning provides a practical basis for targeting interventions, improving P-use efficiency, and supporting sustainable intensification in tropical agroecosystems.

Ethical Approval

Not Applicable

Consent to Participate

Not Applicable

Funding

This research was funded by the European Union's Horizon 2020 Framework Programme under Grant Agreement No. 869200 (Soils4Africa).

Competing Interests

The authors declare that they have no known conflicts of interest.

Availability of data and materials

Data available publicly after the 2026 embargo period

References

https://doi.org/10.5194/egusphere-2026-2815
Preprint. Discussion started: 3 July 2026

Ajiboye, G.A., Ogunwale, J.A., Talbot, J. and Mesele, S.A., 2016. Effect of iron and aluminum oxides fractions and clay type on phosphorus sorption in some alfisols in the Guinea Savanna Ecology of Nigeria. *Nigerian J Soil Environ Res*, *14*, pp.57-67.

Asomaning SK (2020) Processes and factors affecting phosphorus sorption in soils. In: *Sorption in the 2020s*. IntechOpen. https://doi.org/10.5772/intechopen.90719

Bouyoucos, G.J. (1962). Hydrometer method improved for making particle size analyses of soils. *Agronomy Journal*, 54, 464–465.

Breiman, L. (2001). Random Forests. *Machine Learning*, 45, 5–32.

Borggaard OK (1983) Effect of surface area and mineralogy of iron-oxides on their surface-charge and anion-adsorption properties. *Clay and Clay Minerals* 31(3): 230-232

Bouyoucos GJ (1962) Hydrometer method improved for making particle size analyses of soils. *Agronomy Journal* 54:464–465

Buresh RJ, Smithson PC, Hellums DT (1997). Building Soil Phosphorus Capital in Africa. In *Replenishing Soil Fertility in Africa* (eds R.J. Buresh, P.A. Sanchez and F. Calhoun). https://doi.org/10.2136/sssaspecpub51.c6

Doetterl S, Stevens A, Six J, Merckx R, Van Oost K, Casanova Pinto M, Casanova-Katny A, Muñoz C, Boudin M, Zagal E, Boeckx P (2015) Soil carbon storage controlled by interactions between geochemistry and climate. *Nature Geoscience* 8:780–783. https://doi.org/10.1038/ngeo2516

FDALR (1990) *Soils Report. The reconnaissance soil survey of Nigeria (Volume 1-4).* Nigeria. Federal Department of Agriculture and Land Resources, Abuja, Nigeria

Gerard R (2016) Clay minerals iron/aluminum oxides, and their contribution to phosphate sorption in soils – A myth revisited. *Geoderma* 262:213-226

Haynes RJ, Mokolobate MS (2001) Amelioration of Al toxicity and P deficiency in acid soils by additions of organic residues: A critical review of the phenomenon and the mechanisms involved. *Nutrient Cycling in Agroecosystems* 59:47–63

Hendershot WH, Lalande H, Duquette M (1993) Soil reaction and exchangeable acidity. In: Carter MR (ed) *Soil sampling and methods of analysis*. Lewis Publishers, pp 141–145

Hinsinger P (2001) Bioavailability of soil inorganic phosphorus in the rhizosphere as affected by root-induced chemical changes: a review. *Plant and Soil* 237:173–195. https://doi.org/10.1023/A:1013351617532

Hou E, Luo Y, Kuang Y, Chen C, Lu X, Jiang L, Luo X, Wen D (2020) Global meta-analysis shows pervasive phosphorus limitation of terrestrial ecosystems. *Nature Ecology & Evolution* 4:1117–1127. https://doi.org/10.1038/s41559-020-1201-6

Horst WJ, Kamh M, Jibrin JM, Chude VO (2001) Agronomic measures for increasing P availability to crops. *Plant and Soil* 237: 211-223

https://doi.org/10.5194/egusphere-2026-2815
Preprint. Discussion started: 3 July 2026

Huising J, Mesele SA (2022) *Protocol for Field Survey: Guidelines for Field Surveyors on Soil Sample Collection and Field Assessment of Agricultural Lands in Africa.* IITA, 55 p.

Ibia TO, Udo EJ (1993) Phosphorus forms and fixation capacity of representative soils in Akwa Ibom State of Nigeria. *Geoderma* 58:95–106. https://doi.org/10.1016/0016-7061(93)90087-2

IIASA/FAO (2012) *Global agro-ecological zones (GAEZ v3.0)*. IIASA, Laxenburg and FAO, Rome

ISO 10390. (2005). *Soil quality—Determination of pH.* International Organization for Standardization, Geneva.

ISO 11265. (1994). *Soil quality—Determination of electrical conductivity.* International Organization for Standardization, Geneva.

ISO 11277. (2009). *Soil quality—Determination of particle size distribution in mineral soil material—Method by sieving and sedimentation.* International Organization for Standardization, Geneva.

ISO 11464. (2006). *Soil quality—Pretreatment of samples for physico-chemical analysis.* ISO, Geneva.

ISO 17025. (2017). *General requirements for the competence of testing and calibration laboratories.* ISO, Geneva.

Kempen, B., Brus, D.J., De Sousa, L., 2021. Soils4Africa sampling design. Soils4Africa Project Report D3.2B. EU Horizon 2020 Grant agreement ID: 862900. Available at: https://africasis.isric.org/res/files/Soils4Africa_D3.2B_Sampling_design_v01.pdf

Jibrin JM, Chude VO, Horst WJ, Amapu IY (2002) Effect of cover crops, lime, and rock phosphate on maize (*Zea mays* L.) in an acidic soil of Northern Guinea Savanna of Nigeria. *Journal of Agriculture and Rural Development in the Tropics and Subtropics* 103(2):169-176

Kihara J, Bationo A, Waswa B, Kimetu J (2020) Soil fertility management in sub-Saharan Africa: challenges and opportunities. *Agronomy for Sustainable Development* 40:1–19. https://doi.org/10.1007/s13593-020-00607-5

Martens, H., & Naes, T. (1989). *Multivariate Calibration.* John Wiley & Sons.

McLean, E.O. (1965). Aluminum. In: *Methods of Soil Analysis, Part 2* (pp. 978–998). ASA & SSSA.

Mehlich A (1984) Mehlich 3 soil test extractant: a modification of Mehlich 2 extractant. *Communications in Soil Science and Plant Analysis* 15:1409–1416

Menezes-Blackburn D, Giles C, Darch T, George TS, Blackwell MSA, Stutter MI, Shand CA, Lumsdon DG, Cooper P, Wendler R, Brown LK, Almeida DS, Wearing C, Zhang H,

https://doi.org/10.5194/egusphere-2026-2815
Preprint. Discussion started: 3 July 2026

Haygarth PM (2018) Opportunities for improving phosphorus-use efficiency in soils. *Plant and Soil* 427:1–20. https://doi.org/10.1007/s11104-017-3527-2

Mesele, S.A., Ajiboye, G.A. and Talbot, J., 2024. Edaphic factors modulating phosphorus availability in lowland rice systems, Nigeria. *Communications in Soil Science and Plant Analysis*, *55*(19), pp.2935-2951.

Mutwale NM, Jorge F, Chabala LM, Shepande C, Chishala BH, Cambule A, Nhantumbo A, Matague M, Braun M, Sandhage-Hofmann A, Amelung W (2023) Climatic effects on soil phosphorus pools and availability in sub-Saharan Africa. European Journal of Soil Science. https://doi.org/10.1111/ejss.13448

Nelson, D.W., & Sommers, L.E. (1996). Total carbon, organic carbon, and organic matter. In *Methods of Soil Analysis, Part 3* (pp. 961–1010). SSSA.

Osemwotai O, Ogboghodo IA, Aghimien EA (2005) Phosphorus retention in soils of Nigeria – A review. *Agricultural Reviews* 26(2): 148-152

Parfitt, RL (1978) Anion adsorption by soils and soil materials. *Advances in Agronomy* 30:1 - 50

R Core Team (2023) *R: A language and environment for statistical computing*. R Foundation

Reed SC, Yang X, Thornton PE (2015) Incorporating phosphorus cycling into global ecosystem models for climate change research. *Nature Communications* 6:1–8. https://doi.org/10.1038/ncomms7224

Roy R, Fink A, Blair G, Tandon H (2006) *Plant nutrients and basics of plant nutrition. In: Plant Nutrition for Food Security. A guide for Integrated Nutrient Management*. FAO Fertilizer and Plant Nutrition Bulletin, pp 25-42. https://openknowledge.fao.org/handle/20.500.14283/a0443e

Rurinda R, Zingore S, Jibrin JM, Balemi T, Masuki K, Andersson JA, Pampolino MF, Mohammed I, Mutegi J, Kamara AY, Vanlauwe B, Craufurd PQ (2020) Science-based decision support for formulating crop fertilizer recommendations in sub-Saharan Africa. *Agricultural Systems* 180 (2020) 102790. https://doi.org/10.1016/j.agsy.2019.102704

Sanchez PA (2019) Phosphorus. In: *Properties and management of soils in the tropics*. Cambridge University Press, pp 370–414. https://doi.org/10.1017/9781316809785.015

Tamm O (1922) Eine Methode zur Bestimmung der anorganischen Komponenten des Gelkomplexes im Boden. *Meddelanden från Statens Skogsförsöksanstalt* 19:385–404

Tijani MN (2023) Geology of Nigeria. In: Faniran A, Jeje LK, Fashae OA, Olusola AO (eds) *Landscapes and landforms of Nigeria*. Springer, Cham. https://doi.org/10.1007/978-3-031-17972-3_1

Van der Zee SEATM, Van Riemsdijk WH (1988) Model for long-term phosphate reaction kinetics in soil. *Journal of Environmental Quality* 17: 35-41

https://doi.org/10.5194/egusphere-2026-2815
Preprint. Discussion started: 3 July 2026

Vanlauwe B, Coe R, Giller KE (2015) Beyond averages: new approaches to understand heterogeneity and risk of technology success or failure in smallholder farming. *Outlook on Agriculture* 44:229–236. https://doi.org/10.5367/oa.2015.0215

Vitousek PM, Porder S, Houlton BZ, Chadwick OA (2010) Terrestrial phosphorus limitation: mechanisms, implications, and nitrogen–phosphorus interactions. *Ecological Applications* 20:5–15. https://doi.org/10.1890/08-0127.1

Walkley A, Black IA (1934) An examination of the Degtjareff method for determining soil organic matter, and a proposed modification of the chromic acid titration method. *Soil Science* 37:29–38

Yahmed DB (2002) *Atlas of Nigeria*. Editions J.A., Paris

https://doi.org/10.5194/egusphere-2026-2815
Preprint. Discussion started: 3 July 2026

Table 1: Descriptive statistics of the variables by agroecological zones

	Overall N = 1,382	**Derived Savanna N = 363**	**Humid Forest N = 82**	**Northern Guinea Savanna N = 208**	**Sahel Savanna N = 76**	**Southern Guinea Savanna N = 276**	**Sudan Savanna N = 377**
Available P	11.88 ± 5.20	13.63 ± 4.94	15.56 ± 6.79	11.78 ± 5.31	8.99 ± 4.27	12.78 ± 4.64	9.36 ± 4.06
Al_{ox}	594.63 ± 428.01	728.50 ± 441.52	1,295.68 ± 559.95	559.73 ± 294.97	259.14 ± 189.39	626.29 ± 360.44	376.95 ± 267.20
Fe_{ox}	980.79 ± 748.66	1,230.41 ± 797.62	1,666.22 ± 761.24	981.82 ± 564.66	438.48 ± 404.16	1,052.77 ± 696.00	647.42 ± 649.29
pH	5.94 ± 0.42	5.94 ± 0.35	5.31 ± 0.39	6.00 ± 0.41	6.39 ± 0.32	5.89 ± 0.32	6.00 ± 0.43
OC	0.87 ± 0.57	1.21 ± 0.59	1.52 ± 0.48	0.83 ± 0.37	0.27 ± 0.21	0.99 ± 0.47	0.47 ± 0.32
Clay	19.03 ± 13.38	20.64 ± 13.13	30.45 ± 12.81	20.70 ± 13.01	11.82 ± 10.38	19.61 ± 12.99	15.10 ± 12.64
Precipitation (mm)	1,255.29 ± 345.88	1,347.61 ± 168.53	2,191.90 ± 484.35	1,209.11 ± 177.83	714.47 ± 83.66	1,313.26 ± 122.38	1,054.73 ± 170.65
PSI	109.83 ± 86.51	121.18 ± 97.32	184.64 ± 128.24	113.52 ± 70.69	66.80 ± 56.03	111.85 ± 81.56	87.80 ± 66.10

Al_{ox} = Aluminium oxide; Fe_ox = Iron oxide; OC = Organic carbon; PSI = Phosphorus sorption index. Significant differences were observed among the agroecological zones for all variables at $p<0.05$

https://doi.org/10.5194/egusphere-2026-2815
Preprint. Discussion started: 3 July 2026

Table 2 Variation in soil properties by geological formation

Geological Formation	N	Available P (mg kg^{-1})	Al_{ox} (mg kg^{-1})	Fe_{ox} (mg kg^{-1})	pH	Soil organic carbon (%)	Clay (%)	PSI
Abeokuta Formation	7	15.3 ± 4.63	828 ± 214	1250 ± 299	6.1 ± 0.23	1.5 ± 0.40	21.3 ± 9.26	113.62 ± 35.37
Asu River Group	15	11.6 ± 3.58	1161 ± 350	2093 ± 457	5.6 ± 0.33	1.3 ± 0.50	38.8 ± 5.4	238.58 ± 116.47
Awgu-Ndeaboh Shale Group	24	11.1 ± 2.46	661 ± 358	1207 ± 785	5.8 ± 0.29	1.0 ± 0.40	19.9 ± 12.60	132.84 ± 84.78
Basement Complex	616	12.8 ± 5.53	599 ± 305	1020 ± 555	6.0 ± 0.32	1.0 ± 0.51	19.2 ± 10.80	108.77 ± 68.18
Bima Sandstone and Yolde Formation	58	11.5 ± 3.46	505 ± 290	939 ± 584	6.2 ± 0.38	0.8 ± 0.31	18.2 ± 15.18	103.20 ± 77.87
Chad Formation	123	7.8 ± 2.16	219 ± 119	370 ± 258	6.3 ± 0.30	0.2 ± 0.12	9.4 ± 7.47	63.02 ± 43.19
Coastal Plains Sands	33	17.2 ± 6.69	1227 ± 450	1368 ± 371	5.2 ± 0.30	1.4 ± 0.40	25.9 ± 9.15	135.69 ± 51.48
Eze Aku Shale Group	50	11.7 ± 2.78	498 ± 327	875 ± 748	6.0 ± 0.29	0.8 ± 0.47	14.3 ± 10.53	90.05 ± 60.51
Falsebedded Sandstone and Upper Coal Measures	11	12.0 ± 3.86	1253 ± 982	1351 ± 795	5.5 ± 0.30	1.6 ± 0.95	28.0 ± 20.03	232.83 ± 261.51
Gombe Sandstone	21	9.7 ± 2.90	323 ± 154	560 ± 369	6.1 ± 0.19	0.5 ± 0.18	13.8 ± 11.31	79.65 ± 58.10
Gundumi Formation	19	9.1 ± 2.24	281 ± 147	353 ± 205	5.7 ± 0.38	0.3 ± 0.13	11.6 ± 8.38	60.63 ± 34.71
Gwandu Formation	44	8.2 ± 2.20	431± 294	533 ± 349	5.6 ± 0.30	0.4 ± 0.23	17.2 ± 14.02	104.05 ± 83.55
Ilaro Formation	4	15.2 ± 4.72	1036 ± 466	1419 ± 517	6.0 ± 0.36	1.9 ± 0.74	21.3 ± 10.37	141.29 ± 84.63
Illo Formation	28	9.7 ± 2.75	370 ± 166	539 ± 387	5.8 ± 0.22	0.6 ± 0.30	12.4 ± 5.73	79.80 ± 45.49
Imo Clay-Shale Group	7	12.8 ± 5.13	1163 ± 504	1612 ± 537	5.3 ± 0.39	1.3 ± 0.53	35.6 ± 14.94	181.59 ± 59.34
Kerri-Kerri Formation	60	9.2 ± 2.93	292 ± 88	352 ± 171	5.7 ± 0.18	0.4 ± 0.18	9.3 ± 5.14	62.69 ± 31.25
Lignite Formation	8	17.1 ± 5.49	1048 ± 562	1178 ± 467	5.3 ± 0.41	1.3 ± 0.42	21.9 ± 11.04	117.46 ± 68.05
Lower Coal Measures	8	16.2 ± 4.76	940 ± 443	1437 ± 507	6.0 ± 0.57	1.6 ± 0.59	28.1 ± 11.20	116.43 ± 45.88
Marine Facies Lafia Area	8	11.1 ± 2.03	304 ± 75	401 ± 143	6.0 ± 0.15	0.5 ± 0.14	5.6 ± 2.00	50.79 ± 6.23
Nkporo Shale Group	32	12.5 ± 4.44	1274 ± 875	1713 ± 961	5.6 ± 0.54	1.6 ± 0.80	34.4 ± 18.64	223.93 ± 182.74
Nupe Sandstones	48	11.9 ± 3.29	394 ± 137	611 ± 324	6.0 ± 0.15	0.7 ± 0.26	11.4 ± 6.49	70.32 ± 35.16
Pindiga Formation	33	12.9 ± 4.68	793 ± 387	1712 ± 1002	6.6 ± 0.52	0.9 ± 0.33	36.1 ± 18.80	161.76 ± 97.09
Rima Group	28	7.8 ± 2.02	360 ± 238	554 ± 563	5.8 ± 0.54	0.4 ± 0.24	16.6 ± 13.91	93.05 ± 67.81
Sokoto Group	9	13.7 ± 7.87	632 ± 311	984 ± 579	6.0 ± 0.52	0.7 ± 0.45	27.0 ± 17.16	111.44 ± 74.25
Sombreiro Deltaic Plain	4	12.0 ± 3.89	1079 ± 354	1592 ± 401	5.2 ± 0.31	1.5 ± 0.46	27.9 ± 3.95	179.02 ± 16.23
Tertiary to Recent Volcanics	16	18.8 ± 10.13	1282 ± 348	2543 ± 864	6.2 ± 0.70	1.6 ± 0.51	45.0 ± 9.32	181.14 ± 74.98
Younger Granites	13	13.53 ± 3.88	618 ± 330	918 ± 459	6.0 ± 0.49	0.8 ± 0.40	21.0 ± 13.72	95.55 ± 49.98

https://doi.org/10.5194/egusphere-2026-2815
Preprint. Discussion started: 3 July 2026

Table 3: Descriptive statistics of the soil variables by geological Age

Soil Property	**Overall** N = 1,382	**Cretaceous** N = 390	**Jurassic** N = 13	**Pre-Cambrian to Upper Cambrian** N = 616	**Quaternary** N = 214	**Tertiary** N = 149
Available P	11.88 ± 5.20	11.32 ± 3.68	13.53 ± 3.88	12.75 ± 5.53	10.89 ± 5.73	11.00 ± 5.91
Al_{ox}	594.63 ± 428.01	603.57 ± 495.59	618.43 ± 329.62	598.57 ± 304.59	586.63 ± 568.82	564.35 ± 450.00
Fe_{ox}	980.79 ± 748.66	991.25 ± 792.87	918.24 ± 458.49	1,020.16 ± 554.52	966.08 ± 1,053.51	817.23 ± 807.01
pH	5.94 ± 0.42	5.97 ± 0.46	6.01 ± 0.49	5.96 ± 0.32	6.00 ± 0.56	5.73 ± 0.42
OC	0.87 ± 0.57	0.85 ± 0.56	0.84 ± 0.40	0.99 ± 0.51	0.71 ± 0.66	0.68 ± 0.56
Clay	19.03 ± 13.38	19.79 ± 15.62	21.08 ± 13.72	19.17 ± 10.80	17.29 ± 14.05	18.79 ± 15.48
PSI	109.83 ± 86.51	116.65 ± 106.23	95.55 ± 49.98	108.77 ± 68.18	107.14 ± 102.02	101.51 ± 73.87

Al_{ox} = Aluminium oxide; Fe_ox = Iron oxide; OC = Organic carbon; PSI = Phosphorus sorption index. Significant differences were observed among the agroecological zones for all variables at $p<0.05$.

https://doi.org/10.5194/egusphere-2026-2815
Preprint. Discussion started: 3 July 2026

Table 4. Results of the multiple linear regression model predicting log-transformed plant-available phosphorus (P) as a function of soil properties, agroecological zones (AEZ), and geological formations.

Term	Estimate	Standard error	p-value	Lower confidence interval	Higher confidence interval
(Intercept)	0.410	1.059	0.699	-1.668	2.487
log_Al_{ox}	0.016	0.160	0.920	-0.299	0.331
pH	0.018	0.169	0.917	-0.314	0.349
SOC	0.331	0.026	**0.000**	0.279	0.383
Clay	-0.017	0.001	**0.000**	-0.019	-0.015
AEZ:Humid Forest	0.194	0.037	**0.000**	0.122	0.265
AEZ:Northern Guinea	0.011	0.023	0.643	-0.035	0.056
AEZ:Sahel	-0.045	0.041	0.273	-0.126	0.036
AEZ:Southern Guinea	0.046	0.020	**0.025**	0.006	0.086
AEZ:Sudan	-0.026	0.024	0.281	-0.074	0.021
Geology:Jurassic	0.164	0.071	**0.021**	0.025	0.303
Geology:Pre-Cambrian to Upper Cambrian	0.001	0.017	0.940	-0.032	0.034
Geology:Quaternary	-0.005	0.026	0.834	-0.056	0.045
Geology:Tertiary	0.085	0.027	**0.002**	0.032	0.138
log_Al_{ox}:pH	0.052	0.025	**0.041**	0.002	0.101

Coefficients represent estimated effects (β) with standard errors, p-values, and 95% confidence intervals. Continuous predictors include log-transformed oxalate-extractable aluminum (log_Al_{ox}), soil pH, soil organic carbon (SOC), and clay content. Categorical variables (AEZ and geology) are expressed relative to their respective reference categories. The interaction term (log_Al_{ox} × pH) captures the conditional influence of oxide phases on P

https://doi.org/10.5194/egusphere-2026-2815
Preprint. Discussion started: 3 July 2026

availability under varying soil chemical conditions. Significant effects ($p < 0.05$) are highlighted in bold.

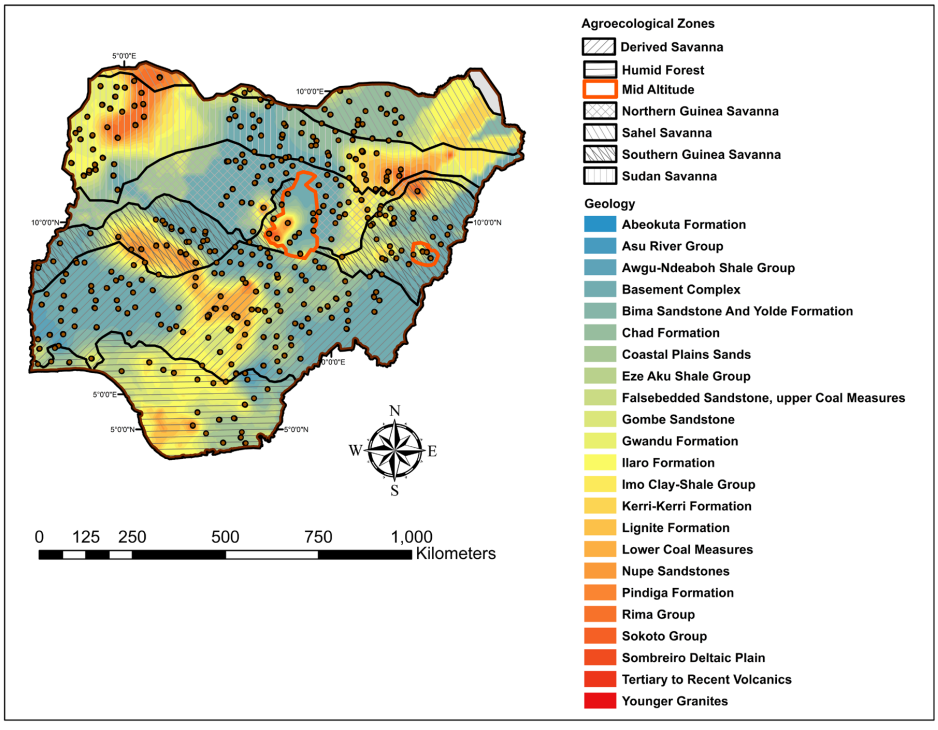

Figure 1. Spatial distribution of soil sampling locations across Nigeria overlaid on agroecological zones and underlying geological formations. Points represent sampled sites, while colored gradients indicate geological units. Agroecological zones are delineated by boundary lines, illustrating the strong climatic and pedogenic gradients across the country.

https://doi.org/10.5194/egusphere-2026-2815
Preprint. Discussion started: 3 July 2026

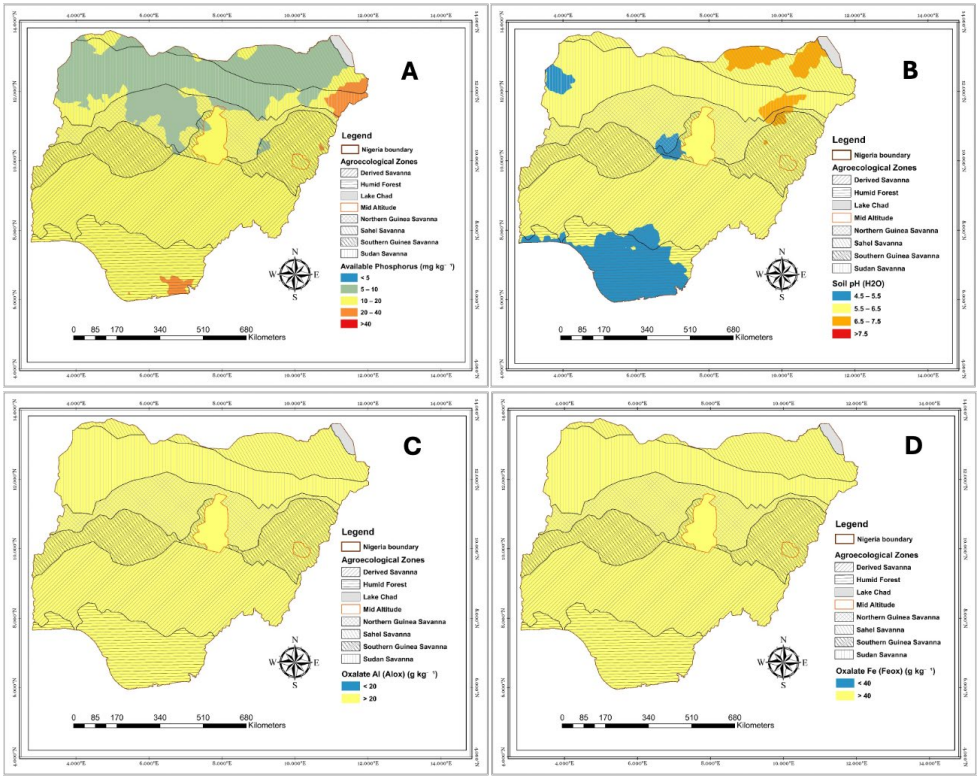

Figure 2. Distribution of available P (A), pH (B), and oxalate-extractable Al (C) and Fe (D) in top soils across Nigeria

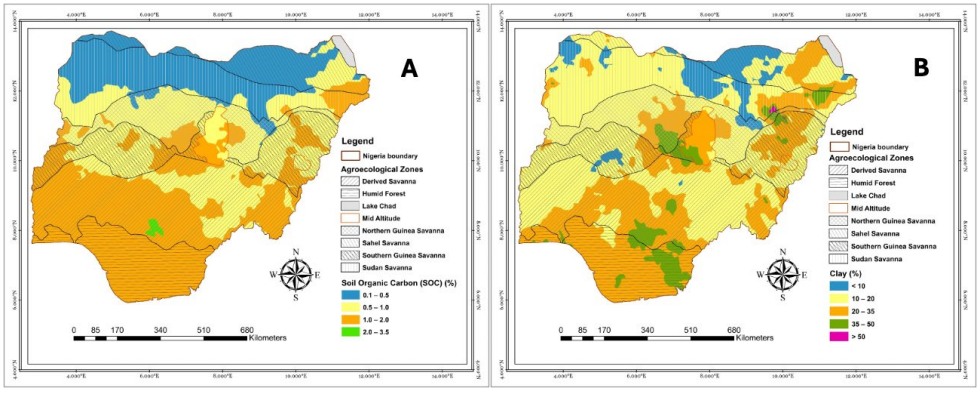

Figure 3: Distribution of SOC (A) and clay (B) in top soils across Nigeria

https://doi.org/10.5194/egusphere-2026-2815
Preprint. Discussion started: 3 July 2026

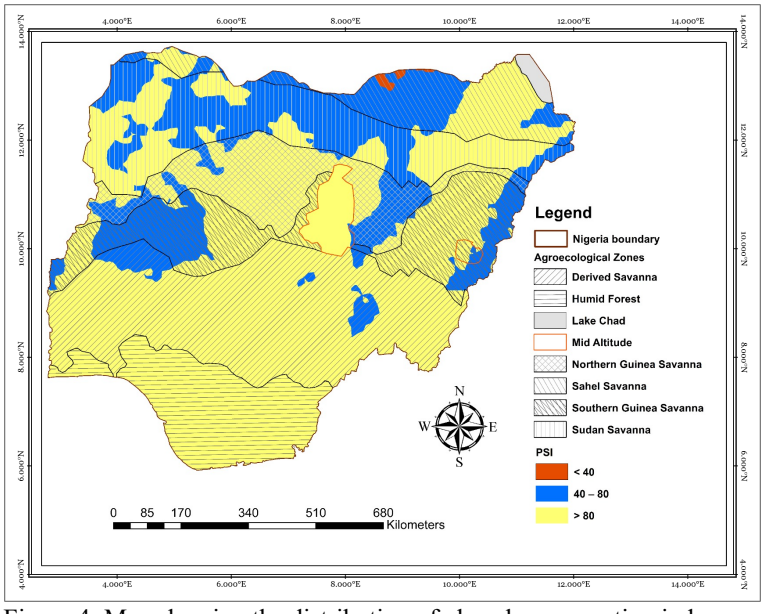

Figure 4: Map showing the distribution of phosphorus sorption index across Nigeria

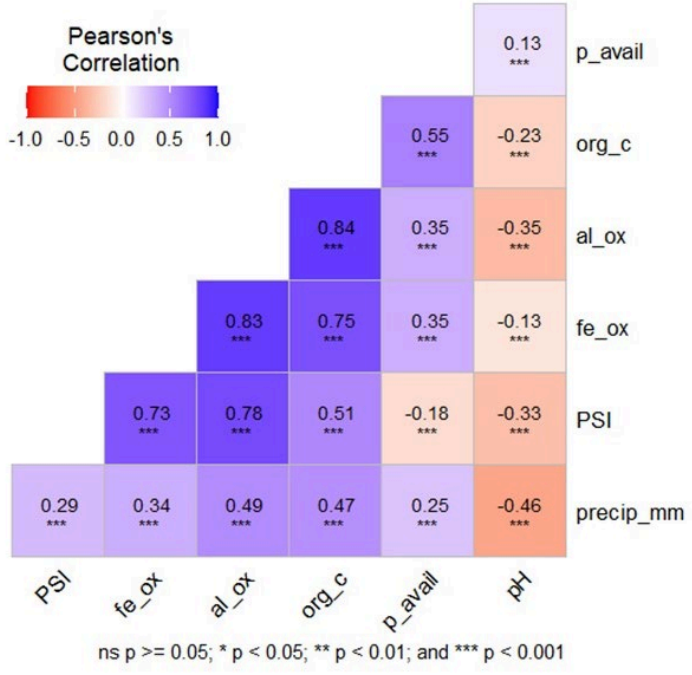

Figure 5: Correlation coefficient among the soil variables. Soil organic carbon (org_c), precipitation (precip_mm), soil pH, oxalate-extractable aluminum (al_ox) and iron (fe_ox), plant-available phosphorus (p_avail), and phosphorus sorption index (PSI). Significant correlations were observed among the variables at $p<0.05$

https://doi.org/10.5194/egusphere-2026-2815
Preprint. Discussion started: 3 July 2026

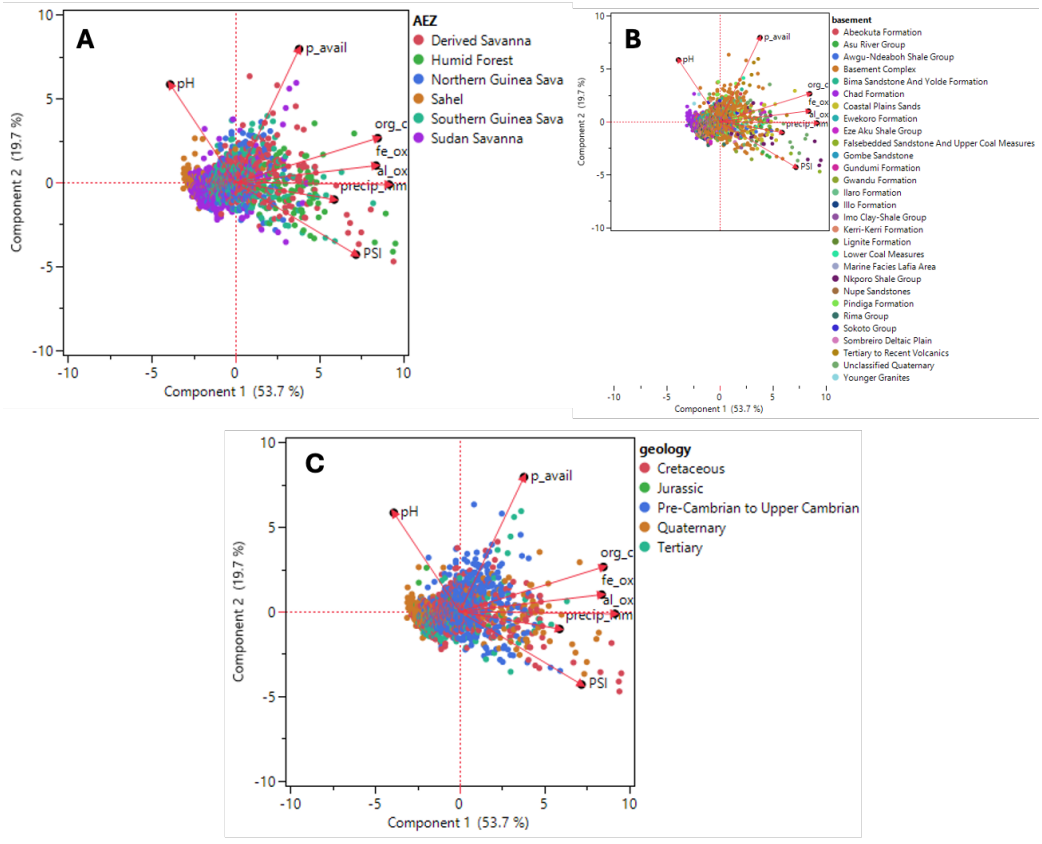

Figure 6: Biplot analysis of the soil variables based on agroecology (A) geological formations (B) and geological age (C). Soil organic carbon (org_c), precipitation (precip_mm), soil pH, oxalate-extractable aluminum (al_ox) and iron (fe_ox), plant-available phosphorus (p_avail), and phosphorus sorption index (PSI).

https://doi.org/10.5194/egusphere-2026-2815
Preprint. Discussion started: 3 July 2026

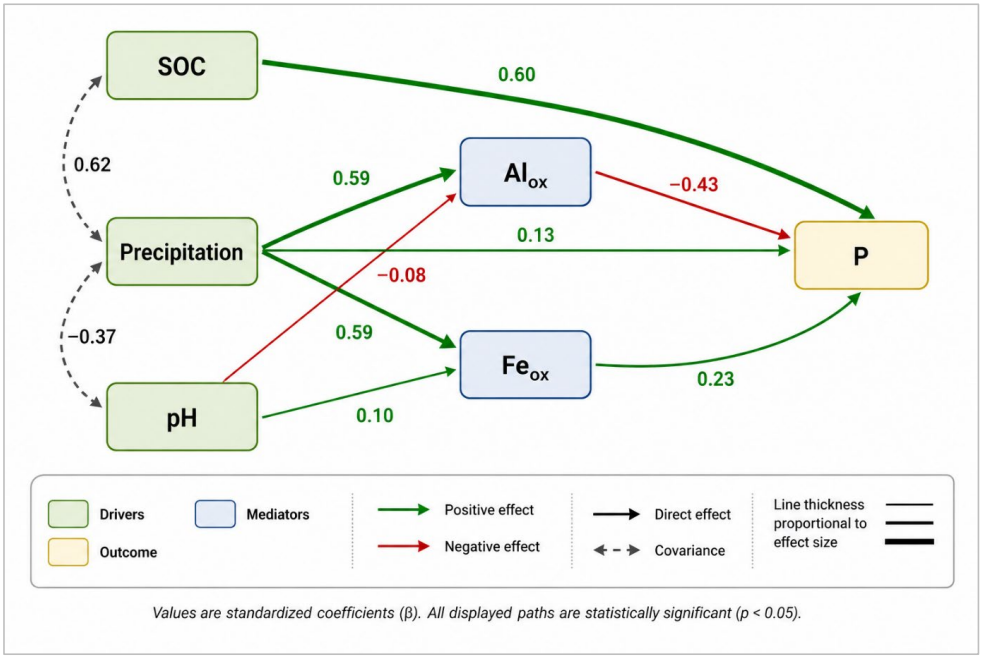

Figure 7: Structural equation model (SEM) illustrating the relationships among soil organic carbon (SOC), precipitation, soil pH, oxalate-extractable aluminum (Al_{ox}) and iron (Fe_{ox}), and plant-available phosphorus (P). Solid arrows indicate direct effects; dashed double-headed arrows represent covariances. Green arrows denote positive relationships, while red arrows indicate negative relationships. Arrow thickness is proportional to the magnitude of standardized path coefficients. Values alongside arrows are standardized coefficients (β). All displayed paths are statistically significant ($p < 0.05$).